

# **Implications of Higher Mode Effects on Seismic Shear Demand of Eccentrically Braced Frames with Short Link Beam**

**Ahmet M. YILDIRIM**<sup>\*1</sup>

**Bilge DORAN**<sup>2</sup>

**Yasin FAHJAN**<sup>3</sup>

## **ABSTRACT**

The capacity design philosophy primarily focuses on limiting the seismic shear force that will affect the structural system and has been widely accepted in the structural earthquake engineering community. However, several sources in the literature indicate that there are still some problematic points in this design philosophy. The main problem is that the proposed solution in this philosophy considers the first fundamental mode of the structural system but overlooks the effects of higher modes. This problem may lead to increased seismic shear force demand that is attempted to be limited by the capacity design philosophy. A similar problem with cantilever walls was first identified in the mid-1970s, and several solutions, which consider both dynamic effects and capacity design principles, were proposed in the relevant literature. Regarding Eccentrically Braced Frames (EBFs) with short link beam, no specific study on the dynamic amplification of shear force demand has been observed in the literature. However, other studies in different contexts have alluded to the possibility of such a phenomenon in EBFs and other steel frames. This study focuses on the dynamic amplification of shear force demands and determines its range using incremental dynamic analysis and multi-modal pushover analyses. Consequently, it has been demonstrated that limiting the shear force demand of the system, as recommended by the capacity design principles in all steel structure design specifications, is not possible. The use of a dynamic amplification factor is suggested to address non-ductile failure modes and enhance structural reliability. In this context, the current study examines the previously mentioned issue for eccentrically braced frames with short link beam in 4-story and 8-story buildings,

---

Note:

- This paper was received on August 30, 2024 and accepted for publication by the Editorial Board on February 24, 2025.
- Discussions on this paper will be accepted by xxxxxxxx xx, xxxx.
- <https://doi.org/>

1 Yildiz Technical University, Department of Civil Engineering, Istanbul, Türkiye  
metin.yildirim@std.yildiz.edu.tr - <https://orcid.org/0000-0003-0501-5239>

2 Yildiz Technical University, Department of Civil Engineering, Istanbul, Türkiye  
doran@yildiz.edu.tr - <https://orcid.org/0000-0001-6703-7279>

2 Istanbul Technical University, Department of Civil Engineering, Istanbul, Türkiye  
fahjan@itu.edu.tr - <https://orcid.org/0000-0003-1254-4526>

\* Corresponding author

representing low-rise and mid-rise buildings respectively. As a result, the seismic shear demands for EBFs found in Incremental Dynamic Analysis are significantly higher than those calculated by using capacity design principles for both 4-story and 8-story buildings. Additionally, the results from Incremental Dynamic Analysis have been comparatively examined with multi-modal pushover analyses. The internal force demands for elements of EBFs, especially in braces, increased due to the higher base shear demands, excluding the link beam.

**Keywords:** Eccentrically braced frames with short link beam, seismic shear demand, push-over analysis, incremental dynamic analysis, higher mode effects, incremental response spectrum analysis.

### **Highlights**

- The study investigated the seismic shear force demand of eccentrically braced steel frames designed using the capacity design method, using two archetypal models representing low and medium-rise buildings.
- Numerous numerical analyses were conducted utilizing various nonlinear analysis methods, including single-mode push-over analysis, incremental dynamic analysis, and incremental response spectrum analysis.
- Significant findings indicate that the capacity design method may not always limit the seismic shear force demand in eccentrically braced steel frames. This is a crucial principle in earthquake-resistant structure design. It was observed that, similar to systems with spine-like structural elements, there could be dynamic amplification effects in addition to the strength presented in the seismic shear force demand.

## **1. INTRODUCTION**

Eccentrically Braced Frames (EBFs) are structures that resist lateral loads, possessing high stiffness in the elastic range and demonstrating significant ductility and energy dissipation in the plastic range. In the EBF system, large eccentricities are intentionally introduced between the brace-to-beam connection and the beam-to-column joint to ensure that the link undergoes yielding in shear. EBFs are typically characterized by a distinct segment of the beam, termed the 'link beam,' which acts as a structural fuse. While ductile steel moment-resisting frames (MRFs) exhibit high ductility but low elastic stiffness, concentrically braced steel frames (CBFs) possess high elastic stiffness but tend to show low ductility due to the braces' buckling failure mode. EBFs effectively bridge this gap by combining the high ductility of MRFs and the elastic stiffness of CBFs. AISC 341 [1] outlines the seismic design method for EBFs, grounded in the capacity design philosophy. This philosophy posits that even when the links of EBFs are fully yielded and have undergone strain-hardening during earthquake events, the other components of the EBFs should retain their elastic properties.

By employing such structural fuses, the seismic shear demand of a building is constrained, aligning with the primary objective of the capacity design philosophy. Ensuring the accurate determination of seismic shear demand is paramount; it guarantees that, as intended, elements other than the link beam remain elastic. However, critiques in the literature highlight certain

shortcomings of this philosophy [2-3]. A fundamental challenge is that the philosophy doesn't fully account for the seismic shear force demand of the structural system, as it doesn't consider the effects of higher modes. This oversight might inadvertently increase the seismic shear force demand that the capacity design philosophy aims to limit. An elevated shear demand could lead to inelasticity in the other EBF elements, potentially causing the structure to unexpectedly collapse an outcome that's highly undesirable in earthquake-resistant design. Initial research on EBFs emerged in Japan during the early 1970s [4-5], where studies concentrated on the behavior of single-story and single-span EBFs under cyclic loads, deriving their force-displacement relationships. In the late 1970s, as a result of many experimental and numerical studies conducted by Popov et al. [6-14], especially the short link beams, it has been observed that the EBFs are very ductile and stable frames for resisting seismic loading.

In recent times, research endeavors concerning EBFs and link beams have primarily centered on the following domains: (1) The effects of material and cross-sectional properties of link beams on overstrength and cyclic behavior, as explored through experimental and numerical studies [15-21]. (2) The development and study of replaceable link beams, with a particular emphasis on bolted variants [22-25]. (3) Investigating the distribution of plastic deformation in multi-story buildings designed per the capacity design principles [26-33]. Outside these prevalent areas of study, literature on the collapse probability of EBFs is relatively sparse. Notably, a recent contribution to this niche topic was made by Qi et al. [34].

Despite the occurrence of the 1994 Northridge and 1995 Kobe earthquakes, detailed insights into the earthquake performance of EBFs remained scant. However, the 2010 and 2011 earthquakes in New Zealand provided an opportunity for extensive observations regarding the behaviors of EBFs during seismic events. Post-earthquake evaluations [35-36] highlighted EBFs in buildings of various heights 2, 3, 5, 12, and 22-storeys. These EBFs were either standalone or paired with steel moment-resisting frame systems and precast reinforced concrete systems. Notably, these structures exhibited pronounced plastic deformation demands on bond beams, with a few link beams even displaying cracks. Yet, no local or global collapses were reported for the buildings in question. Gardiner et al. [36] observed that the structures had withstood loads approximately double their original design specifications, still outperforming the current design benchmarks by about 1.7 times. The lone exception was a fracture in one link. The observed increase in seismic shear force demand, compared to the design level, suggests possible reasons. Overstrength in materials and systems is a likely contributor. Yet, the dynamic influence on shear force demand, potentially causing a rise in seismic load, is another pivotal area for discussion.

The dynamic amplification of seismic shear demand on cantilever walls was first identified by Blakeley et al. (1975) in the mid-1970s. In designing shear walls, the wall's flexural capacity is determined by considering overstrength, in alignment with capacity design principles. This capacity is used to find an inverted triangle load distribution which is similar to first mode shape. An additional concentrated load of 0.1 times the base shear is applied at the top of the wall to consider higher mode effects. However, Blakeley et al. [2] noted that during significant earthquakes, inertial forces, which are predominantly first mode until a flexural hinge forms at the base, undergo redistribution and are increasingly influenced by higher modes. Consequently, the locus of inertial force distribution can deviate, sitting either below or above the anticipated inverted triangle force distribution. This variance can lead to

the seismic shear demand at the wall's base or top being substantially higher than the stipulated design values. Indeed, after a plastic hinge emerges at the base of a cantilevered RC wall, inertia forces are redistributed within this transformed system, which can be conceptualized as a combination of a plastic hinge and an elastic spine (as depicted in Fig.1 - Case 2). Here, the elastic spine refers to the elastic behavior of the main lateral load-resisting system and represents the elastic portion of the structure, excluding the plastic hinges, in the mechanism formed after plastic hinging occurs. A similar phenomenon has been observed in strongback braced systems, as documented by Simpson [37].

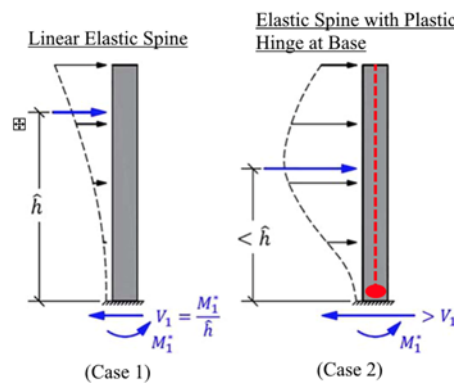


Fig. 1 - The inertia force distribution in before and after plastic hinge formation [37].

If an analogy is established between cantilever walls and EBFs, it's observed that after the formation of shear plastic hinges in all, or the majority of, link beams, the distribution of inertial forces changes. This shift results in higher mode contributions becoming dominant instead of the first mode. MacRae [38] found a greater base shear demand in response history analyses than the expected global base shear capacity of the considered EBF archetypes. MacRae [38] also attributed this increase to the changing distribution of lateral inertial forces. A schematic explanation of the changing lateral load distribution is shown in Fig. 2.

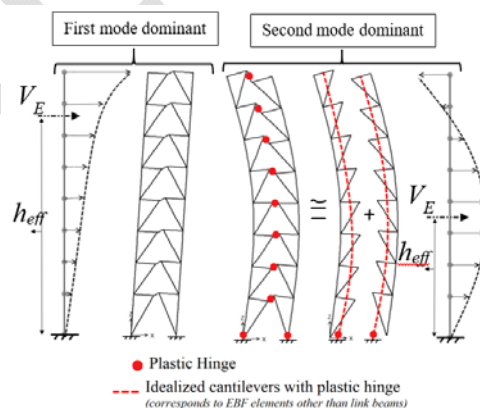


Fig. 2 - Change of inertial force distribution after yielding of all link beams and column base.

This paper initially focuses on the upper limits of seismic shear demands using three-dimensional (3D) push-over analysis (POA), which considers the first mode shape of buildings for load distribution. The results are then compared with the seismic shear demand computed using Incremental Dynamic Analysis (IDA). Furthermore, Incremental Response Spectrum Analysis (IRSA) is included in this study to verify the IDA results and to determine the modal contribution to inertial forces.

All analyses have been performed on 4 and 8-story EBF (Eccentrically Braced Frame) archetypes, which were designed as part of a study conducted by NIST.TN.1863-3 [39]. In this study, several nonlinear dynamic analyses were carried out on these archetypes. It was found that the axial forces on the columns and braces of these structures are higher than those calculated using capacity design principles. It's important to note that an increase in these axial forces corresponds to an increase in seismic shear demand. NIST.TN.1863-3 [39] concluded that this might result from the link beam calibration with experimental test results, which indicated approximately a 15% higher overstrength than the  $1.25 \times V_{pe}$  ( $V_{pe} = R_y \times V_p$ ) used in the design as per AISC 341. However, Richards [40] argued that the increase in column axial forces cannot be solely explained by strain hardening and overstrength. Due to higher internal force demands than those calculated with the capacity design principle, some elements (such as columns and braces) that were intended to remain elastic experienced inelasticity. This issue was identified by Koboevic et al. [29-30] through nonlinear time history analyses on buildings with varying numbers of stories. Similar results were also obtained by Crişan and Stratan [28]. This study aims to investigate the amplification of shear force demand due to nonlinear higher mode effects in EBFs.

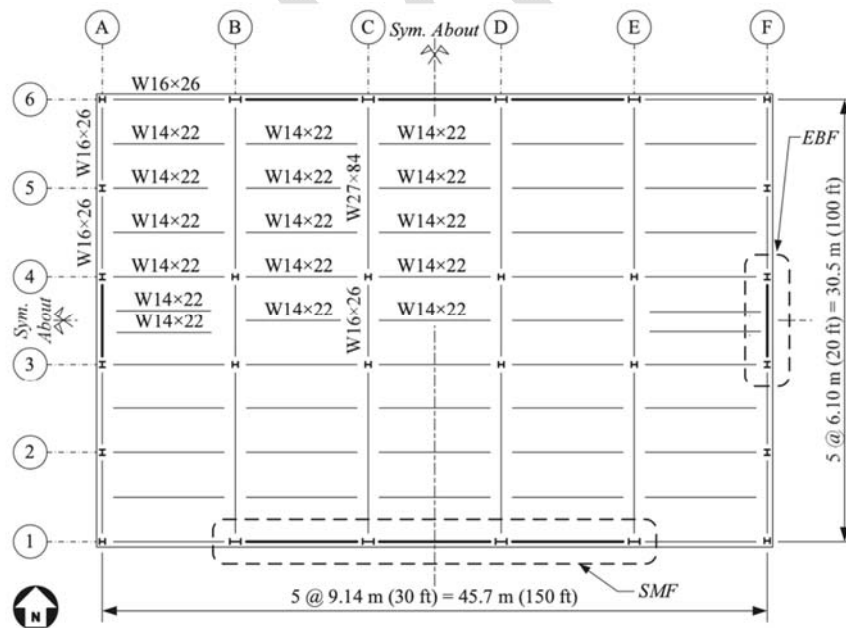


Fig. 3 - Typical floor plan.

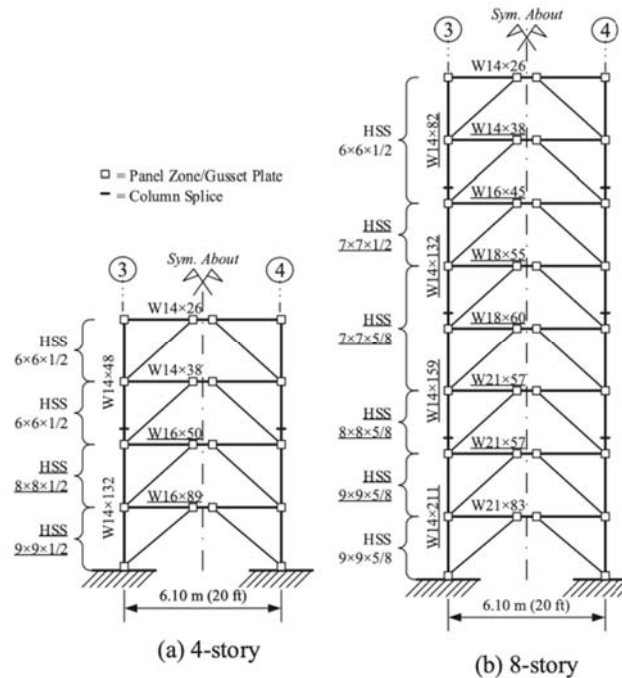


Fig. 4 - EBF elevations for the (a) 4-story, (b) 8-story.

## 2. MODELING AND ANALYSIS

### 2.1. Archetype Models and Seismic Design Parameters

The 4 and 8-story buildings used in this study are based on the report NIST.TN.1863-3 [39] prepared by Speicher and Harris. They were designed using the Equivalent Lateral Force (ELF) method for floors other than the ground floor in both buildings. The width of linked bays ( $L$ ) within the EBFs is 6.1 m, and the link length ( $e$ ) is 0.76 m, giving an  $e/L$  ratio of roughly 0.13. The building floor plan and EBF elevations are illustrated in Figs. 3-4. The story heights are 5.486 m for the first floor and 4.267 m for the other floors. The column and beam cross-sections are wide flange US sections, while the brace cross-sections are tubular. Seismic force resistance in the N-S direction is provided by two perimeter EBFs, and in the E-W direction, Special Moment Frames are used as the seismic force resisting system. Seismic analysis and design parameters are presented in Table 1. The EBFs were designed in compliance with the seismic design requirements set forth in ASCE 7-10 [42] and AISC 341-10 [1]. The section compactness and capacity design requirements specified in AISC 341-10 [1] determined the brace sizes and initial column sizes. For the 8-story building, the plastic link rotation limits defined in AISC 341-10 [1] were the governing factor for column sizes. Due to the prescribed lateral force distribution in ASCE 7-10 [42], the elastic lateral drift of a slender braced frame can be more influenced by the global flexural mode of deformation rather than the shear mode. Drift and rotation angles taken from ASCE 7-10 and

AISC 341-10 are 2% and 8%, respectively. The analysis and design procedure described in the NIST.TN.1863-3 [39] report is illustrated in Fig. 5.

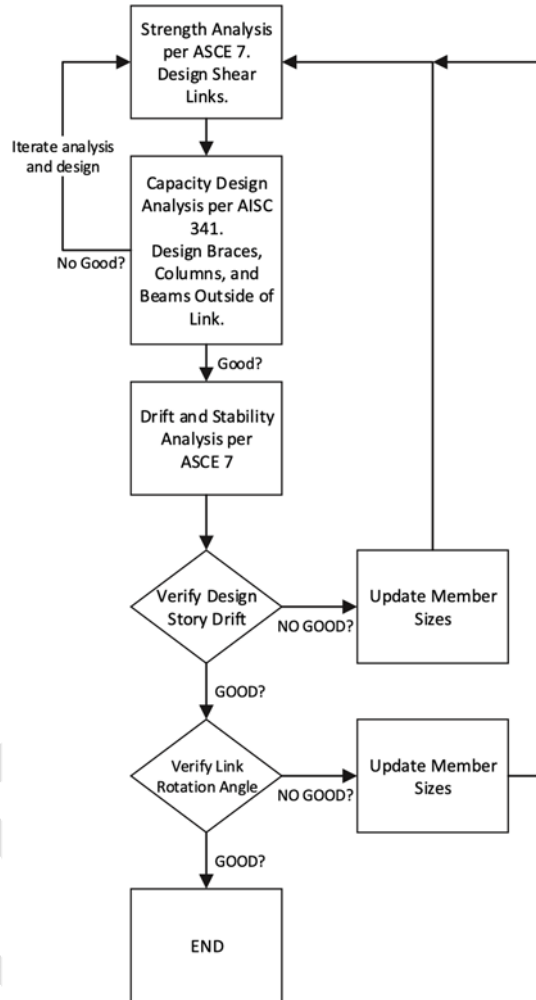


Fig. 5 - Flow chart of EBF design process [39].

The Effective Length Method, as outlined in AISC 360 §C1 [43], is used for the design of EBF elements, excluding the link beam. The effective length factor,  $K$ , was conservatively set as '1' to determine the nominal compression strength of these elements. The Redundancy Factor ( $\rho$ ), equal to 1.3 for a single bay in the Seismic Force Resisting System (SFRS) as per ASCE 7-10 §12.3.4 [42], was however neglected in the design to minimize member overstrength contributions in the seismic performance assessment [44]. A minimum link depth of 14 inches (W14) was selected for connection constructability, which contributes to

the design overstrength of link beams in the upper stories where story shear demands are relatively low. HSS sections are used as braces in the 4- and 8-story archetype buildings. The link plastic rotation is determined using the design story drift, calculated by amplifying the results of an elastic analysis. This provides a rough estimate of actual expected drifts. The inelastic drift can be calculated using the formula  $\Delta_{in} = (C_d - 1)\Delta_e$ , where  $C_d$  is the deflection amplification factor, set at 4 for eccentrically braced frames;  $\Delta_e$  is the drift from an elastic analysis using the prescribed base shear; and  $\Delta_{in}$  is the inelastic drift [45].

*Table 1 - Seismic analysis and design parameters.*

Parameters	4-story	8-story
$S_s$	1.50 g	1.50 g
$S_1$	0.60 g	0.60 g
$F_a$	1.00	1.00
$F_v$	1.50	1.50
$S_{DS}$	1.00 g	1.00 g
$S_{D1}$	0.60 g	0.60 g
Site Class	D	D
$C_U T_a$	0.90 sec	1.48 sec
$T_{comp.}$	1.04 sec	2.14 sec
Analysis Procedure	ELF	ELF
R, $C_d$ , $\Omega_0$	8, 4, 2	8, 4, 2
Importance Factor, I	1.00	1.00
Total Building Weight, W	22830 kN	47000 kN
Design Base Shear, V	1890 kN	2375 kN

## 2.2. Nonlinear Modelling and Analyses

Push-Over Analysis (POA) and Incremental Dynamic Analysis (IDA) of EBFs have been conducted using 3D models in the PERFORM-3D software [46], aiming to investigate the nonlinear higher mode effects on shear force demand. To ensure comparability with the NIST.TN.1863-3 [39] study, the following assumptions and simplifications were made during modeling and analysis: (1) Beam ends, as well as braces, are fixed to the column to approximate the gusset plate restraint; (2) The stiffness of the gusset plate connection is estimated by doubling the adjacent member stiffnesses over an estimated plate length of 0.46 m; (3) Floor slabs are modeled as semi-rigid membrane diaphragms with no out-of-plane bending stiffness and a 0.5 in-plane stiffness modifier to account for cracking at design loading, and the out-of-plane stiffness of the concrete deck is neglected; (4) Gravity load-carrying framing is modeled to capture P-Delta ( $P-\Delta$ ) effects; (5) The gravity beams are modeled with pinned connections to minimize their strength and stiffness contributions to the seismic performance of the EBFs.

The model comprises linear frame elements and nonlinear discrete plastic hinges (located at the ends of columns, braces, beams outside the link, and at the middle of link beams). The plastic shear hinge model, taken from the report NIST.TN.1863-3 [39], has been calibrated with test data from that report and verified with the numerical model proposed in this study (see Fig. 6 and Fig.7). The shear hinge force-deformation model proposed by Speicher and Harris [44] follows a tri-linear backbone curve with limited hardening behavior, as provided in PERFORM-3D [46]. In past research on the nonlinear behavior of EBFs, the plastic shear hinge model developed by Ramadan and Ghobarah [47], or similar models, have been widely used. The key difference between the model used in this research, as proposed by Speicher and Harris [44], and the one developed by Ramadan and Ghobarah [47], lies in the definition of strain hardening; in the former, hardening is not limited and increases at a certain rate, while in this present study, hardening is limited. Consequently, the shear force demands likely to occur in the link beam are restricted at high earthquake intensities.

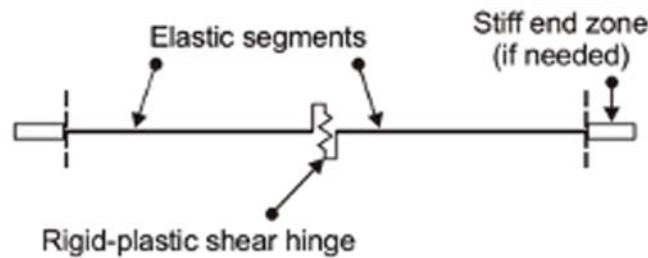


Fig. 6 - Frame element model for shear link

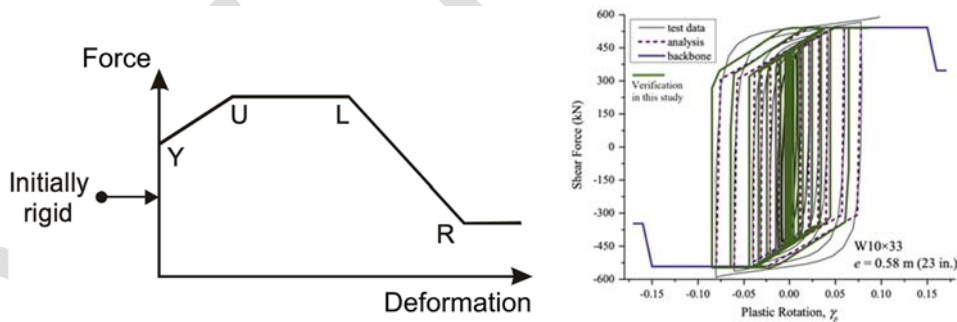


Fig. 7 - Shear link component backbone curves in PERFORM-3D (left), shear link hinge model calibration (right) [39].

The elements of the EBFs, except for the link beam, are modeled using moment-rotation hinges with axial interaction (i.e., PMM hinges see Fig. 8). These hinges have been assigned to the ends of the beams outside the link, as well as to the columns and braces, in order to capture potential nonlinearities in these members. Additionally, a nonlinear panel zone component model in PERFORM-3D [46] is utilized for the beam-to-column joint (see Fig.

9). The overall nonlinear modelling of the elements of the EBFs, except for the link beam schematically described in Fig. 10.

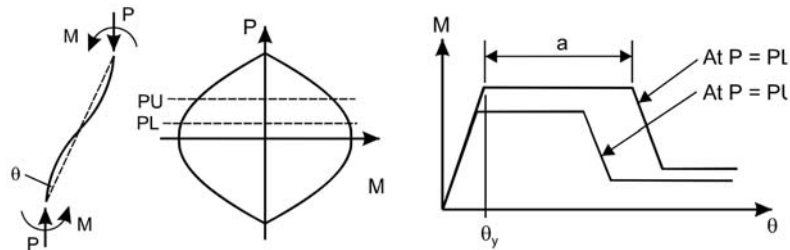


Fig. 8 - PMM Hinge (Steel Rotation Type) schematic definition in Perform 3D

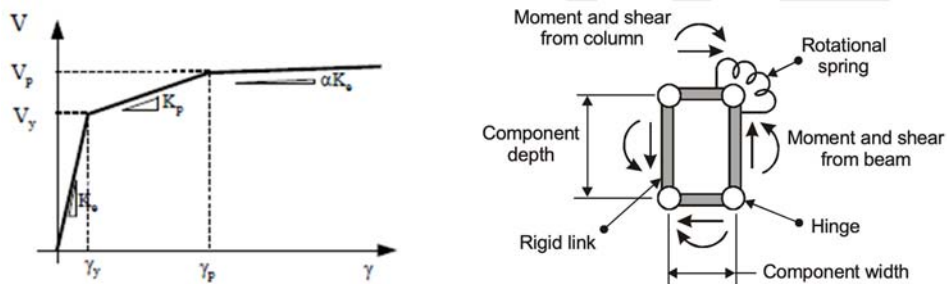


Fig. 9 - Panel zone force-deformation relationship (left), model for panel zone component (right)

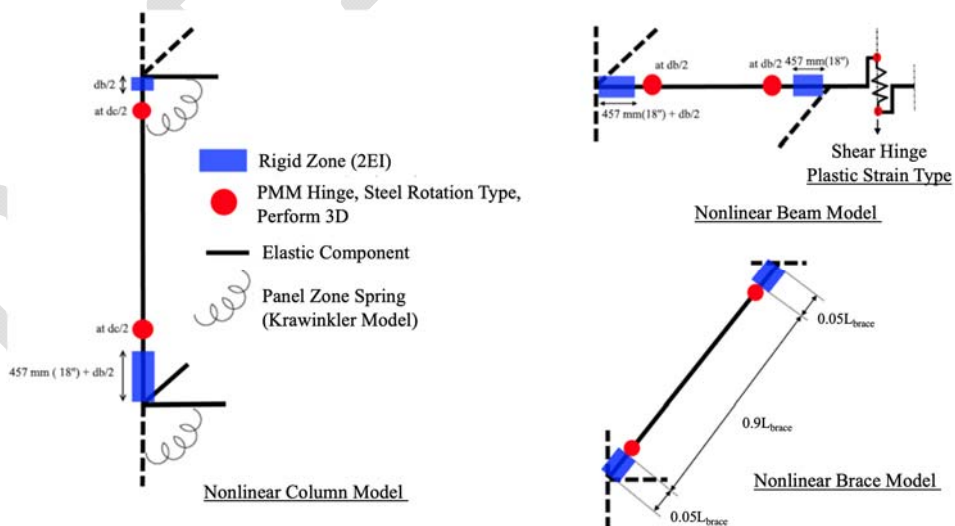


Fig. 10 - Nonlinear models for all EBF elements except the link beam.

POA has been performed using Fajfar's N2 method [48], while Vamvatsikos and Cornell's approach [49] was adopted for IDA. This analysis method offers seismic demand and capacity prediction through nonlinear dynamic analyses with scaled ground motion records. According to Vamvatsikos and Cornell [49], IDA data can enhance understanding of structural behavior and the relationship between static and dynamic responses. In this study, IDA curves showing roof displacement versus base shear are plotted for the archetype buildings, allowing comparison within the same coordinate system. The ground motion records used are from the NIST.TN.1863-3 report [39].

### 3. ANALYSIS RESULTS AND DISCUSSION

#### 3.1. Seismic Base Shear Demand Calculation Using Capacity Design Principles

The variation of shear forces is illustrated in Fig.11, showing results from: (1) conducting a linear analysis using the Equivalent Lateral Force (ELF) method, (2) using the design shear strengths of the link beams as per AISC 341 [1] formulation, and (3) using the ultimate strengths of the link beams. Accordingly, following capacity design principles, the seismic base shear capacity of the archetype building can be calculated by summing the story shear forces, excluding the effect of the strength of the column-to-base connection. In Fig.11, story strengths are determined as  $V_{i,story} = \sum V_i \times L_b / h_{sx}$  where  $L_b$  is the bay width,  $h_{sx}$  is the story height, and  $V_i$  is the design shear strength (design or ultimate) of the link.

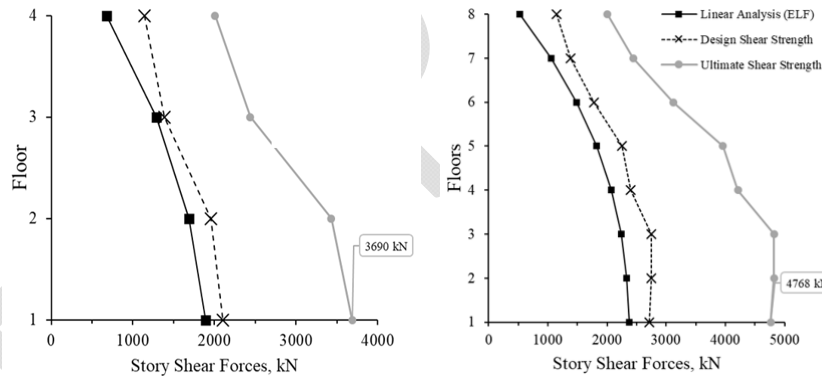


Fig. 11 - Story shear forces corresponds to ELF analysis and story strengths obtained with capacity design principles.

#### 3.2. Push-over Analysis

The maximum seismic base shear capacity (limit) of the archetype buildings, designed in accordance with AISC 341 [1], has been determined using first mode-based 3D POA. The corresponding pushover curves are presented in Fig.12. The POA results from this study align well with those previously obtained by Speicher and Harris [44]. For the maximum base shear limit, values of 4099 kN for the 4-story building and 4800 kN for the 8-story building have been determined through POA. It is noteworthy that the values reported by Speicher and Harris [44] were 4087 kN and 4747 kN, respectively.

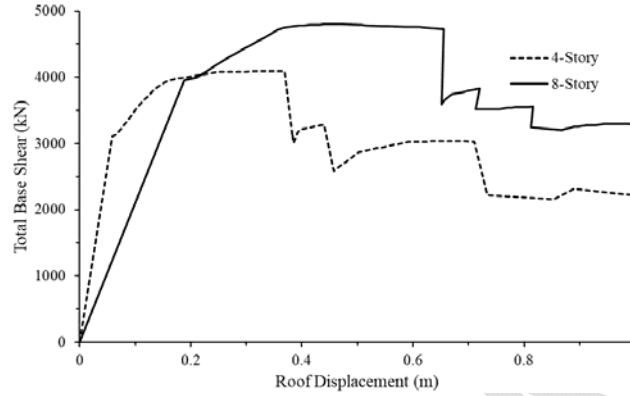


Fig. 12 - Push-over curves.

The top displacement demands of the archetype buildings have been determined using the N2 method [48] and are compared with the values obtained by Speicher and Harris in the NIST.TN.1863-3 report [39], as shown in Table 2. Additionally, these results will be compared with the IDA results discussed in Section 3.3.

Table 2 - Top displacement demands corresponding to seismic hazard levels (DBE and MCE).

Hazard Level	NIST.TN.1863-3		Present Study	
	4 - story	8 - story	4 - story	8 - story
$\Delta_{DBE}$ (m)	0.203	0.426	0.207	0.460
$\Delta_{MCE}$ (m)	0.305	0.640	0.313	0.693

Top displacement demands have also been compared with the results from NIST.TN.1863-3 [39], as shown in Table 2, and the maximum difference is about 7 percent between the mentioned study and the current study. This difference is considered acceptable, given that a different method (the N2 method) has been used in this study.

### 3.3. Incremental Dynamic Analysis

Within the IDA approach, nonlinear time-history dynamic analyses are carried out using a set of earthquake ground motions scaled to specific intensity levels. These ground motions are scaled using a factor that increases in certain increments (e.g., 0.05g, 0.1g). The IDA analysis for the archetype buildings has been conducted by applying the methodology proposed by Vamvatsikos and Cornell [49]. The ground motion records are listed in Table 3, and the elastic acceleration spectra, along with the code design spectra, are displayed in Fig. 13.

Top displacements and base shear values obtained from both IDA and POA are plotted in the same coordinate system in Figs. 14 and 15 for the 4-story and 8-story buildings, respectively. The ratio of the seismic base shear demand obtained in the IDA results to the maximum seismic base shear capacity determined in the POA is defined as the dynamic shear amplification ( $\beta_d$ ).  $\beta_d$  values are calculated considering both the maximum and mean of the IDA results for each archetype at certain target top displacements, which are obtained in the POA conducted for Maximum Considered Earthquake (MCE) and Design Based Earthquake (DBE) hazard levels.

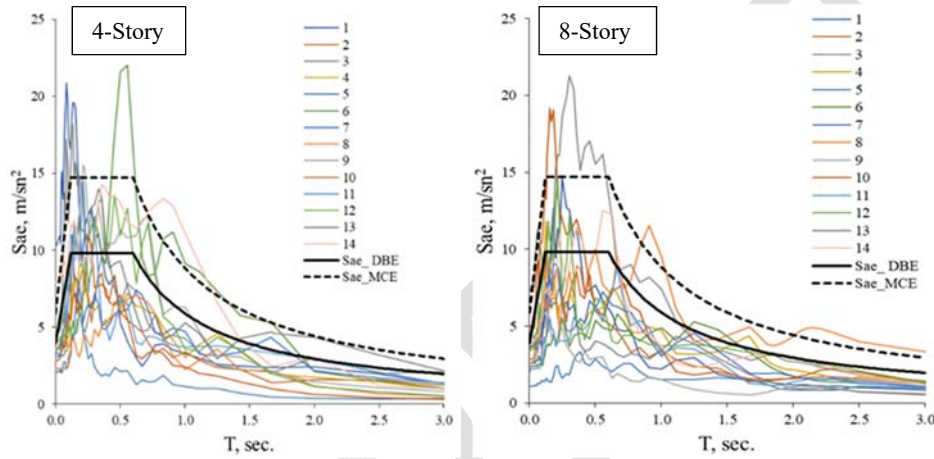


Fig. 13. Elastic acceleration spectra of selected ground motion records with code design spectra.

Table 3 - Ground motion records used in this study [39].

4 - Story Building				8 - Story Building			
ID	Event Name	Station	Component	ID	Event Name	Station	Component
1	Cape Mendocino	Cape Mendocino	2	1	Imperial Valley	El Centro Array #11	2
2	Superstition Hills	Poe Road (temp)	2	2	Superstition Hills	Poe Road (temp)	2
3	Kocaeli, Turkey	Duzce	1	3	Duzce, Turkey	Bolu	1
4	Superstition Hills	El Centro Imp. Co.	1	4	Imperial Valley	Delta	2
5	Kocaeli, Turkey	Arcelik	1	5	Kocaeli, Turkey	Arcelik	2
6	Northridge	Beverly Hills - Mulhol	2	6	Landers	Yermo Fire Station	1
7	Imperial Valley	Delta	2	7	Superstition Hills	El Centro Imp. Co.	1
8	Kobe, Japan	Shin-Osaka	2	8	Chi-Chi, Taiwan	CHY101	2
9	Northridge	Canyon Country-WLC	2	9	San Fernando	LA - Hollywood Stor	2
10	Friuli, Italy	Tolmezzo	1	10	Manjil, Iran	Abbar	1
11	Loma Prieta	Gilroy Array #3	2	11	Kobe, Japan	Shin-Osaka	1
12	Landers	Coolwater	2	12	Loma Prieta	Gilroy Array #3	2
13	Manjil, Iran	Abbar	2	13	Hector Mine	Hector	1
14	Duzce, Turkey	Bolu	2	14	Northridge	Canyon Country-WLC	1

As observed in Figs. 14-15, the 4-story building retains its maximum base shear capacity at the MCE (Maximum Considered Earthquake) level, whereas the 8-story building does not,

experiencing a loss of about 25 percent of its maximum capacity. However, the performance evaluation of EBFs, as previously conducted in the technical report NIST.TN.1863-3 [39], is not within the scope of this study.

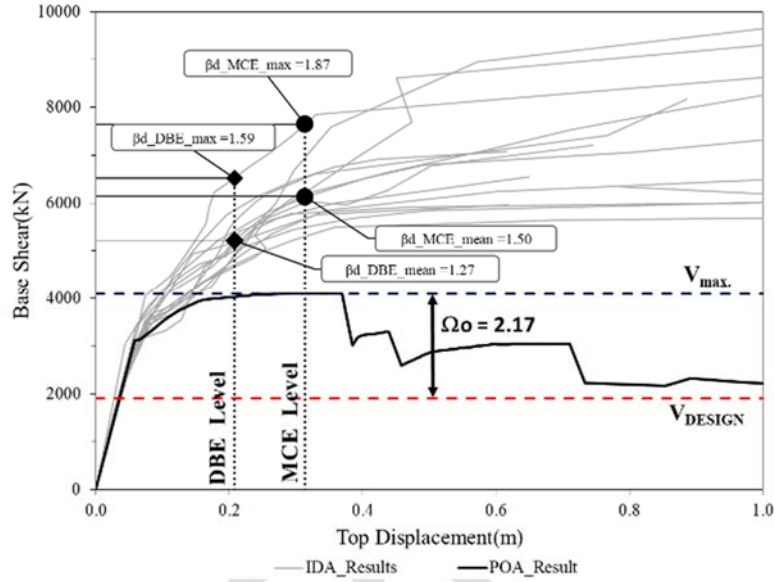


Fig. 14 - Capacity curves for 4-story building with the POA and IDA.

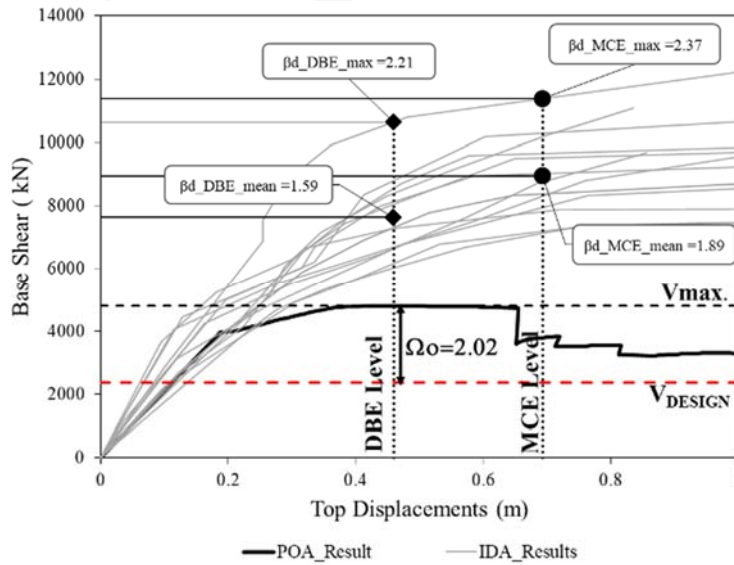


Fig. 15 - Capacity curves for 8-story building with the POA and IDA.

The seismic shear demands of EBFs found in the IDA are significantly higher than those in the POA. A statistical summary of the  $\beta_d$  values calculated at DBE and MCE levels is provided in Table 4. The seismic shear demands for both the 4-story and 8-story buildings, as determined by capacity design principles, POA, and IDA, are shown in Figs. 14-15 for comparison. All the story shear demands determined by IDA correspond to the DBE hazard level. It is evident from Fig. 16 that the story shear demands according to the mean of the IDA results are higher than those calculated by capacity design principles, particularly in the lower stories.

Due to the calibration of the shear hinge model with test data, the ultimate shear strength ( $1.25R_yV_p$ ) of the link beam, as defined in AISC 341-10 [1], increases by 15 percent, as stated in NIST TN 1863-3 [39]. In this study, this increase is considered in both the pushover analysis (POA) and capacity design calculations. Therefore, the dynamic shear amplification obtained using incremental dynamic analysis (IDA) is refined to exclude any effects of overstrengthening and hardening. Concurrently, the shear link hinge model does not allow unlimited isotropic strain hardening. As a result, the dynamic amplification of story shear and internal force demands becomes evident in the results since the effect of calibration and unlimited isotropic hardening effect on  $\beta_d$  was excluded. Hence, the internal force demand in the EBFs elements, other than the link beam, is also expected to increase due to the dynamically amplified seismic shear demand. Although these elements are designed to remain elastic, the increase in internal force demand might lead to inelastic deformation demands.

Speicher and Harris [44], in their analyses for NIST.TN.1863-3 [39], observed an increase in axial force demand on columns and braces, attributing this to the calibration of the link beam with test data. However, Richards [40] suggested that the increase in column axial forces cannot be solely explained by strain hardening and overstrength. In our study, the calibrated hinge model is used, aiming to observe further amplification of seismic demand due to dynamic effects. The normalized axial force demands of columns and braces determined by the aforementioned analysis methods are illustrated in Figs. 17 -18.

Table 4 - Statistical Summary of IDA results.

$\beta_d$ for 4-story				
	Max.	Min.	Mean	Mean+1 std.
DBE	1.59	1.14	1.27	1.40
MCE	1.87	1.29	1.50	1.65
$\beta_d$ for 8-story				
	Max.	Min.	Mean	Mean+1 std.
DBE	2.21	1.26	1.59	1.85
MCE	2.37	1.48	1.86	2.12

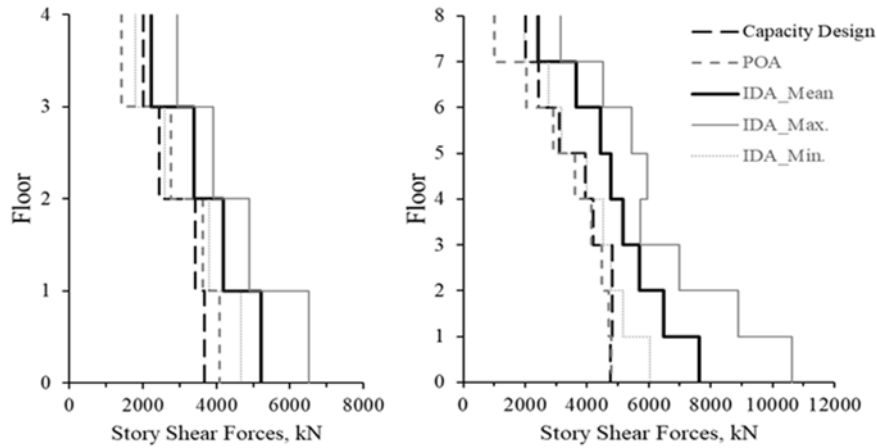


Fig. 16 - Story shear forces.

In Figs. 17-18, the axial force demands ( $P_u$ ) obtained from the mentioned analyses are normalized against the axial demand ( $P_e$ ) under the Equivalent Lateral Force (ELF) and presented according to the floor levels. In the determination of axial force demand in columns using capacity design calculations, AISC permits the multiplication of the ultimate link beam capacity by 0.88. However, this value was not applied in the capacity design analysis conducted in this study. The mean results of IDA and capacity design calculations show that the column axial force demands take similar values on the lower floors, while the values obtained with capacity design are lower than those from IDA in the upper stories. Nevertheless, when examining the curve in Figs. 14-15 corresponding to the maximum IDA results (at the DBE hazard level), it is observed that the axial force demands of the columns attain higher values.

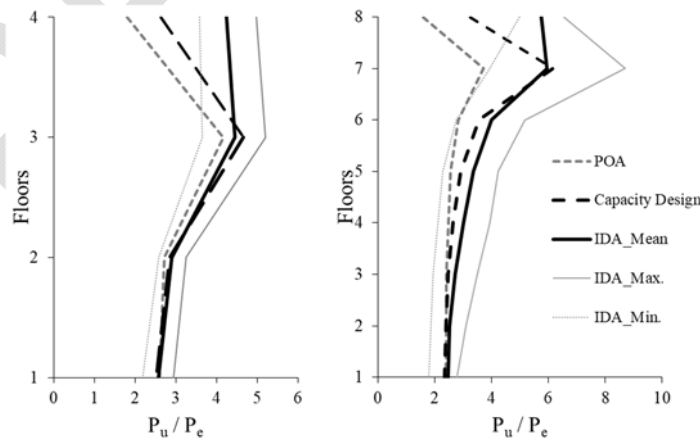


Fig.17 - Normalized column axial forces.

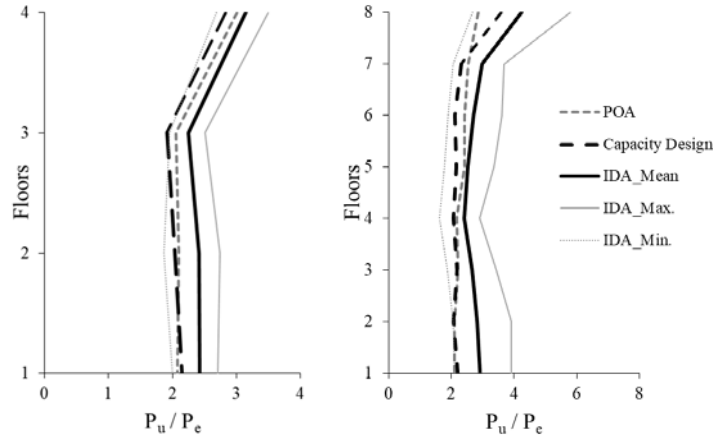


Fig. 18 - Normalized brace axial forces.

It is posited, based on observations from this study, that this increase could be attributable to dynamic shear amplification. Given that braces are the primary elements for transferring story shears, it is anticipated that their axial force demands of braces would be significantly influenced by the dynamic shear amplification. As depicted in Fig. 18, the axial demands of braces, corresponding to the mean of IDA results, are notably higher than those calculated using the capacity design principle. While this difference is consistent across all floors in 4-story buildings, it is found to be considerably larger in the lower and upper floors of 8-story buildings.

### 3.4. Incremental Response Spectrum Analysis

The contribution of different modes to seismic demand can be investigated using various modal decomposition methods. In this context, as graphically depicted in Fig. 19, each mode can hypothetically be considered to have its own hysteresis loop and modal capacity diagram. Modal parameters, such as periods, modal participation factors, and other generic response parameters of the structure, can be calculated at each time step of a time history analysis, taking into account both material and geometric nonlinearities. Using these nonlinear parameters, the equivalent static forces for each mode can be separately determined, allowing for an assessment of the contribution of higher modes to the inertia force distribution. Simpson [37] employed a similar method in her research on strongback braced frame systems. Alternatively, multi-mode push-over analysis can be used to evaluate the contribution of higher modes to the inertia force distribution. While there are different types of multi-mode push-over analysis, the Incremental Response Spectrum Analysis method (IRSA) [50] was employed in this study.

IRSA method is a multi-mode push-over analysis technique recommended for evaluating and designing buildings and bridges under seismic effects [50]. As illustrated graphically in Fig. 20, IRSA is developed as a process in which modal displacements are calculated incrementally until they reach their peak values, referred to as the inelastic spectral

displacements for each mode. This is achieved by applying a piecewise linear Response Spectrum Analysis (RSA) at each incremental step between the formation of two consecutive plastic hinges. With the modal displacement increments for each mode at each step, increments of all response quantities of interest, such as story displacements, story drifts, plastic hinge rotations, and internal forces, can be calculated using an appropriate modal combination rule. In the practical application of IRSA, the well-known equal displacement rule is employed, and the earthquake input is represented as an elastic response spectrum [50]. In this study, the method was used to examine the seismic shear force demands originating from higher modes in a more practical manner.

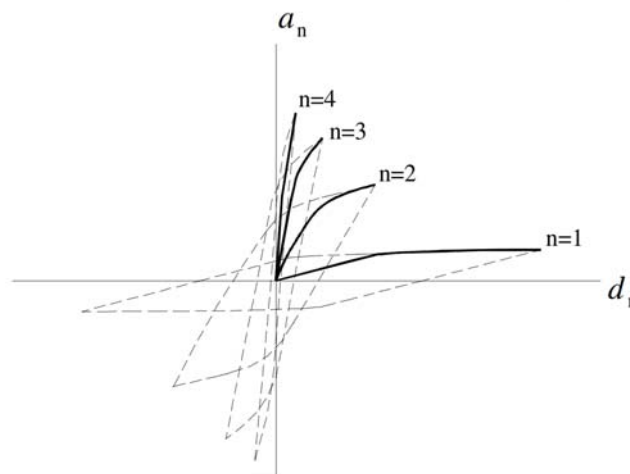


*Fig. 19 - Hypothetic hysteresis loops and modal capacity diagrams (solid black lines) [50].*

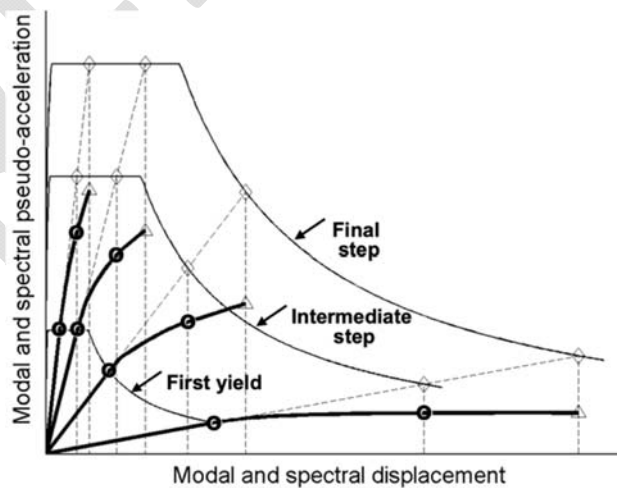


*Fig. 20 - Scaling the modal displacements by monotonically increasing the response spectrum [50].*

Incremental spectrum analysis was utilized in a practical manner within the scope of this study, thanks to several assumptions listed below:

- a. Only the first two modes were considered in the IRSA analysis.
- b. The P-delta effect has been neglected. Given that this effect is not a significant factor in low-rise and braced structures, its omission is not expected to have a serious impact on the analysis of seismic shear force demand. In Fig. 21 presents a comparative analysis of thrust curves obtained from IRSA and POA analyses. The results from IRSA Mode 1 are sufficiently consistent with the POA results. It is clear that there is no significant impact of neglected P-delta effect in the context of seismic shear demand, which is the main subject of this study.

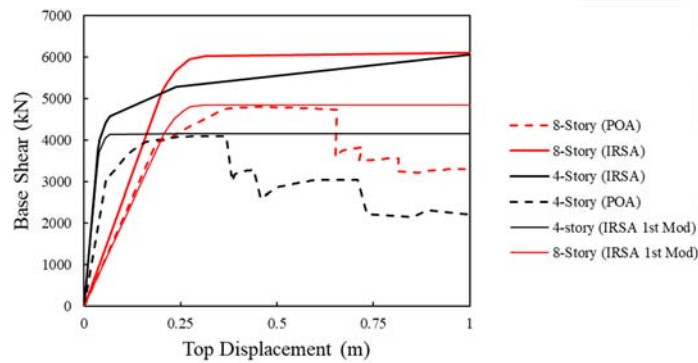


Fig. 21 - Comparison of POA and IRSA curves.

- c. The locations of plastic hinges are assumed to be fixed, corresponding to the mechanism state of the 1st mode. This assumption is consistent with the principles of capacity design.
- d. A bilinear elasto-plastic hinge model has been employed for the inelastic behavior of the link beam, where the hardening effect is not considered, and the ultimate shear capacity is specified to be equivalent to that described in Section 2.2 for the plastic hinge model.
- e. The potential plastic yielding in the braces has been disregarded, as the design is based on capacity design principles, which typically account for such effects.
- f. IRSA analyses were conducted with 2D (planar) model.

In the Fig. 22. modal capacity diagrams for both modes obtained as a result of IRSA, as well as the pushover curves for each mode, are presented separately. Additionally, the pushover curve representing the combined effects of all modes, calculated using the SRSS method, is also provided. The curves referred to as Modal Capacity Diagram in Fig. 22. represent the spectral acceleration and spectral displacement capacities of single-degree-of-freedom systems corresponding to different modes of the structure.

In Table 5, a comparison of the base shear forces obtained from all analyses is presented, and based on the results of the pushover analyses, a comparison factor ( $\beta_k$ ) has been calculated.

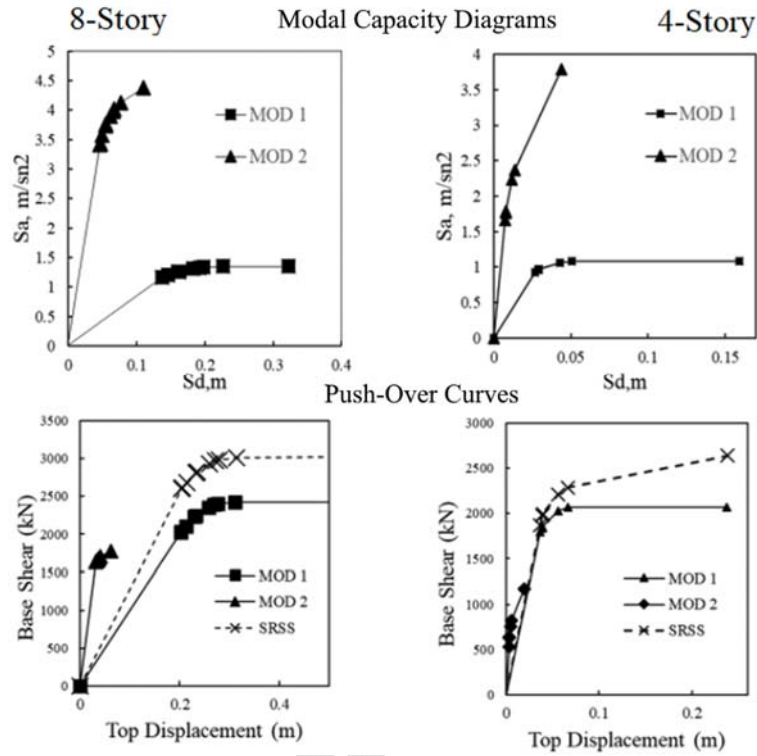


Fig. 22 - Modal capacity diagrams and push-over curves yielded from IRSA.

Table 5 - Seismic shear demand comparison.

Analysis Types	4-story		8-story	
	V (kN)	$\beta_k$	V (kN)	$\beta_k$
-	4099	1.000	4800	1.000
IDA (DBE)	5220	1.273	7632	1.590
IRSA (DBE)	5277	1.287	6180	1.288
IRSA (First Mode)	4144	1.011	4851	1.010

#### 4. CONCLUSIONS

In this study, the seismic shear demand of the 4- story and 8-story frames, designed in a previous study, has been investigated using POA and several IDA analyses for comparison. The effect of the reinforced concrete slab's strength and stiffness on the building system's lateral stiffness was not considered, focusing instead on the bare frame behavior. This scenario is representative of a real structure where shear studs are not used in the concrete slab in the link beam zone. The maximum seismic shear demands from IDA were compared

with the capacity curve (push-over curve) at both DBE and MCE hazard levels. Additionally, the column and brace axial force demands from IDA and POA were normalized by the elastic axial force (ELF) for comparison with the axial demand calculated using the capacity design principle. Therefore, this study also examined seismic shear amplification in EBFs and its impact on internal forces, particularly axial forces. The conclusions derived from this study are as follows:

- (1) Although the capacity design method is practical and logical, it does not completely reflect the seismic behavior of EBFs, as indicated in the literature, due to reasons such as: (1) non-uniform distribution of link beam rotation over the structure height; (2) inelastic deformation demands on EBF elements other than the link beams; (3) higher column axial demands than those calculated using capacity design principles.
- (2) The seismic shear demands for EBFs found in IDA are significantly higher than those calculated using capacity design principles for both 4-story and 8-story buildings. On average, dynamic amplifications of 1.27 and 1.59 for the DBE level, and 1.5 and 1.86 for the MCE level were found for 4-story and 8-story buildings, respectively. Additionally, maximum and minimum values of 1.87 and 2.37, respectively, were found for both structures. This increase in seismic shear demands also results in amplified internal forces demand on columns, braces, and beams outside the links. It is suggested that a dynamic amplification factor be proposed for EBFs, as given in design codes for cantilever shear walls, in the design of EBFs, to prevent dynamic instability.
- (3) The variation in the distribution of inertial forces with high mode effects and the corresponding increase in shear force have been determined for different steel braced frames in current studies. This situation, detected in this study, was confirmed by IRSA, and values similar to those obtained in response to the IDA results specified in the previous point were found.
- (4) The impact of seismic shear amplification in EBFs on the axial force demands of braces and columns was also examined in this study. It was observed that this amplification had a more pronounced effect on the axial force demands of the braces than on the columns. Considering these results, separate dynamic amplification coefficients can be suggested for columns and braces.
- (5) This study was conducted with a limited number of archetype buildings and ground motion records to enable a comparative study with Speicher and Harris [44]. Varying dynamic shear amplification factors were found in IDA for different ground motion records. This amplification depends on the dynamic characteristics of both the ground motion records and the archetypes. An extensive study encompassing all aspects affecting the dynamic characteristics of both ground motion records and archetypes could be carried out as further research.

### References

- [1] ANSI/AISC 341-10 (2010), Seismic provisions for structural steel buildings, American Institute of Steel Construction: Chicago, IL, USA.

- [2] Blakeley, R.W.G., Cooney, R.C. and Megget, L.M. (1975), "Seismic shear loading at flexural capacity in cantilever wall structures." *Bull. of the NZ Soc. for Earthquake Eng.*, 8(4), 278-290.
- [3] Rutenberg A. (2013), "Seismic shear forces on RC walls: review and bibliography." *B. Earthq. Eng.* 11(5), 1727-1751. <https://doi.org/10.1007/s10518-013-9464-1>
- [4] Fujimoto M., Aoyagi T., Ukai K., Wada A. and Saito K. (1972), "Structural characteristics of eccentric K-Braced frames," *Tans. Arch. Inst. Jap.*, 195(), 39-49, (in Japanese)
- [5] Tanabashi, R., Naneta, K. and Ishida, T. (1974), "On the rigidity and ductility of steel bracing assemblage", *Proceedings of the 5th World Conference on Earthquake Engineering, Rome, Italy.*
- [6] Roeder C.W. and Popov E.P. (1977), "Inelastic Behavior of Eccentrically Braced Steel Frames Under Cyclic Loading", Report No. UCB/EERC-77/18, University of California, Berkeley, CAL, USA.
- [7] Roeder, C.W.; Popov, E.P., (1978), "Eccentrically braced steel frames for earthquakes", *Journal of the Structural Division*, 104(ST3),391-412.
- [8] Roeder, C.W., Popov, E.P., (1978), "Cyclic shear yielding of wide flange Beams", *J. Eng. Mech. Div.*, 104(4):763-780.
- [9] Roeder, C.W., Foutch, D.A., Goel, S.C. (1987), "Seismic testing of full-scale steel building-part II", *J. Struct. Eng.*, 113(11):2130-2145. [https://doi.org/10.1061/\(ASCE\)0733-9445\(1987\)113:11\(2130\)](https://doi.org/10.1061/(ASCE)0733-9445(1987)113:11(2130))
- [10] Hjelmstad K.D., Popov, E.P., (1983), "Cyclic behavior and design of link beams", *J. Struct. Eng.*, 109(10):2387-2403. [https://doi.org/10.1061/\(ASCE\)0733-9445\(1983\)109:10\(2387\)](https://doi.org/10.1061/(ASCE)0733-9445(1983)109:10(2387))
- [11] Malley, J.O.; Popov, E.P., (1984), "Shear Links in Eccentrically Braced Frames", *J. Struct. Eng.*, 110(9), 2275-2295. [https://doi.org/10.1061/\(ASCE\)0733-9445\(1984\)110:9\(2275\)](https://doi.org/10.1061/(ASCE)0733-9445(1984)110:9(2275))
- [12] Kasai, K.; Popov, E.P., (1986(a)), "Cyclic web buckling control for shear link beams", *J. Struct. Eng.*, 112(3),505-523. [https://doi.org/10.1061/\(ASCE\)0733-9445\(1986\)112:3\(505\)](https://doi.org/10.1061/(ASCE)0733-9445(1986)112:3(505))
- [13] Kasai, K.; Popov, E.P., (1986(b)), "General behavior of WF steel shear link beams", *J. Struct. Eng.*, 112(2),362-382. [https://doi.org/10.1061/\(ASCE\)0733-9445\(1986\)112:2\(362\)](https://doi.org/10.1061/(ASCE)0733-9445(1986)112:2(362))
- [14] Ricles, J.M.; Popov, E.P., (1989), "Composite action in eccentrically braced frames", *J. Struct. Eng.*, 115(8), 2046-2066. [https://doi.org/10.1061/\(ASCE\)0733-9445\(1989\)115:8\(2046\)](https://doi.org/10.1061/(ASCE)0733-9445(1989)115:8(2046))
- [15] Okazaki T., Arce G., Ryu H.C. and Engelhardt M.D. (2005), "Experimental study of local buckling, overstrength, and fracture of links in eccentrically braced frames", *J. Struct. Eng.*, 131(10), 1526-1535. [https://doi.org/10.1061/\(ASCE\)0733-9445\(2005\)131:10\(1526\)](https://doi.org/10.1061/(ASCE)0733-9445(2005)131:10(1526))

- [16] Richards, P.W. and Uang, C.M., (2005), "Effect of flange width thickness ratio on eccentrically braced frames link rotation capacity", *J. Struct. Eng.*, 131(10), 1546-1552. [https://doi.org/10.1061/\(ASCE\)0733-9445\(2005\)131:10\(1546\)](https://doi.org/10.1061/(ASCE)0733-9445(2005)131:10(1546))
- [17] Dusicka P., Itani A.M. and Buckle I.G. (2010), "Cyclic behavior of shear links of various grades of plate steel", *J. Struct. Eng.*, 136(4), 370-378. [https://doi.org/10.1061/\(ASCE\)ST.1943-541X.0000131](https://doi.org/10.1061/(ASCE)ST.1943-541X.0000131)
- [18] Ashtari, A. and Erfani, S. (2016), "An analytical model for shear links in eccentrically braced frames", *Steel Compos. Struct., Int. J.*, 22(3), 627-645. <https://doi.org/10.12989/scs.2016.22.3.627>
- [19] Lian, M., Su, M. and Guo, Y. (2015), "Seismic performance of eccentrically braced frames with high strength steel combination", *Steel Compos. Struct., Int. J.*, 18(6), 1517-1539. <https://doi.org/10.12989/scs.2015.18.6.1517>
- [20] Caprili, S., Mussini, N. and Salvatore, W. (2018), "Experimental and numerical assessment of EBF structures with shear links", *Steel Compos. Struct., Int. J.*, 28(2), 123-138. <https://doi.org/10.12989/scs.2018.28.2.123>
- [21] Li, T., Su, M. and Sui, Y. (2020), "Spatial substructure hybrid simulation tests of high-strength steel composite Y-eccentrically braced frames", *Steel Compos. Struct., Int. J.*, 34(5), 715-723-1539. <https://doi.org/10.12989/scs.2020.34.5.715>
- [22] Stratan A. and Dubina D. (2004), "Bolted links for eccentrically braced steel frames", *Proceedings of the 5th AISC/ECCS International Workshop: Connections in Steel Structures V. Behaviour, Strength and Design*, Delft, The Netherlands, June.
- [23] Mansour, N., Christopoulos, C. and Tremblay R. (2011), "Experimental validation of replaceable shear links for eccentrically braced steel frames", *J. Struct. Eng.*, 137(10)1141-1152. [https://doi.org/10.1061/\(ASCE\)ST.1943-541X.0000350](https://doi.org/10.1061/(ASCE)ST.1943-541X.0000350)
- [24] Fussell A.J., Cowie K.A., Clifton G.C., and Mago N. (2014), "Development and research of eccentrically braced frames with replaceable active links", *Proceedings of the 2014 NZSEE Conference*, Auckland, New Zealand, March.
- [25] Bozkurt, M. B. And Topkaya, C. (2017), "Replaceable links with direct brace attachments for eccentrically braced frames", *Eartq. Eng. Struct. D.*, 46(13), pp.2121-2139. <https://doi.org/10.1002/eqe.2896>
- [26] Popov, E.P., Kasai, K. and Ricles, J.M. (1992), "Methodology for optimum EBF link design", *Earthquake Engineering Tenth World Conference*, Madrid, Spain, July.
- [27] Bosco, M., Rossi, P.P. (2009), "Seismic behavior of eccentrically braced frames", *Eng. Struct.*, 31(3), 664-674. <https://doi.org/10.1016/j.engstruct.2008.11.002>
- [28] Crişan, A., Staratan, A. (2009), "Overstrength demands in multistorey eccentrically braced frames", *Proceedings of the 11th WSEAS International Conference on Sustainability in Science Engineering*, Timisoara, Romania, May.

- [29] Koboevic, S., Rozon, J. and Tremblay R. (2012), "Seismic performance of low-to-moderate height eccentrically braced steel frames designed for North American seismic conditions", *J. Struct. Eng.*, 138(12),1465-1476, 2012. [https://doi.org/10.1061/\(ASCE\)ST.1943-541X.0000433](https://doi.org/10.1061/(ASCE)ST.1943-541X.0000433)
- [30] Koboevic, S. and David, S.O.J. (2010), "Design and seismic behavior of taller eccentrically braced frames", *Can. J. Civ. Eng.*, 37(2), 195-208. <https://doi.org/10.1139/L09-131>
- [31] Chen, L., Tremblay, R. and Tirca, L. (2012), "Seismic performance of modular braced frames for multi-story building applications", *Earthquake Engineering*, 15. World Conference of Earthquake Engineering, Lisboa, Portugal, September.
- [32] Chen, L., Tremblay R. and Tirca L. (2014), "Enhancing the seismic performance of multi-story buildings with a modular tied braced frame system with added energy dissipating devices", *International Journal of High-Rise Buildings*, 3(1), 21-33.
- [33] Kuşyılmaz A. and Topkaya C. (2016), "Evaluation of seismic response factors for eccentrically braced frames using FEMA P695 methodology", *Earthq. Spectra* 32(1) 303-321. <https://doi.org/10.1193/071014EQS097M>
- [34] Qi, Y., Li, W. and Feng, N. (2017), "Seismic collapse probability of eccentrically braced steel frames", *Steel Compos. Struct., Int. J.*, 24(1), 37-52. <https://doi.org/10.12989/scs.2017.24.1.037>
- [35] Clifton, C., Bruneau, M., MacRae, G., Leon, R., and Fussell, A. (2011), "Steel structures damage from the Christchurch earthquake of February 22, 2011, NZST.", *Bull. New Zealand Soc. Earthquake Eng.*, 44(4), 297-318.
- [36] Gardiner G., Clifton C., and MacRae G.A. (2013), "Performance, damage assessment and repair of a multistory eccentrically braced frame building following the Christchurch earthquake series", *Proceedings of the Steel Innovations Conference 2013, Christchurch, New Zealand, February.*
- [37] Simpson B. (2020), "Higher-mode force response in multi-story strongback-braced frames", *Earthquake Engineering and Structural Dynamics*, 49(14), 1406-1427.
- [38] MacRae, G. (1989), "The seismic response of steel frames" Ph.D. Dissertation, University of Canterbury, Christchurch.
- [39] Harris, J.L., Speicher, M.S. (2015) "Assessment of first-generation performance-based seismic design methods for new steel buildings. Eccentrically braced frames" Report no. NIST.TN.1863-3, National Institute of Standards and Technology, Gaithersburg, MD,USA.
- [40] Richards, P.W.(2009), "Seismic column demands in ductile braced frames", *J. Struct. Eng.*, 135(1), 33-41. [https://doi.org/10.1061/\(ASCE\)0733-9445\(2009\)135:1\(33\)](https://doi.org/10.1061/(ASCE)0733-9445(2009)135:1(33))
- [41] ASCE/SEI (2006), *Seismic Rehabilitation of Existing Buildings*, Structural Engineering Institute of the American Society of Civil Engineers; Reston, VA, USA.
- [42] ASCE 7 (2010), *Minimum Design Loads for Buildings and Other Structures*, American Society of Civil Engineers and Structural Engineering Institute, Reston, VA, USA.

- [43] ANSI/AISC 360-10 (2010), Specification for Structural Steel Buildings; American Institute of Steel Construction, Chicago, IL, USA.
- [44] Speicher, M.S. and Harris, J.L., (2016), "Collapse prevention seismic performance assessment of new eccentrically braced frames using ASCE 41", *Eng. Struct.*, 117, 344-357. <https://doi.org/10.1016/j.engstruct.2016.02.018>
- [45] Bruneau M., Uang C.M., and Sabelli R. (2011), *Ductile Design of Steel Structures*, McGrawHill, New York, NY, USA.
- [46] PERFORM 3D (2018), *Nonlinear Analysis and Performance Assessment for 3D Structures Ver.7.0.0.*; Computers and Structures Inc., Berkeley, CA, USA.
- [47] Ramadan, T., and Ghobarah, A. (1995), "Analytical model for shear-link behavior", *J.Struct.Eng.*, 121(11), 1574-1580. [https://doi.org/10.1061/\(ASCE\)0733-9445\(1995\)121:11\(1574\)](https://doi.org/10.1061/(ASCE)0733-9445(1995)121:11(1574))
- [48] Fajfar, P. (2000), "A nonlinear analysis method for performance-based seismic design", *Earthq. Spectra*, 16(3), 573-592. <https://doi.org/10.1193/1.1586128>
- [49] Vamvatsikos, D., Cornell, C.A. (2002) "Incremental dynamic analysis", *Eartq. Eng. Struct. D.*, 31(3),491-514. <https://doi.org/10.1002/eqe.141>
- [50] Aydinoglu, M. N. (2003). An incremental response spectrum analysis procedure based on inelastic spectral displacements for multi-mode seismic performance evaluation. *Bulletin of Earthquake Engineering*, 1(1), 3-36. <https://doi.org/10.1023/A:1024853326383>